Cosmic Evolution and Galaxy Formation: Structure, Interactions, and Feedback
ASP Conference Series, Vol. 3×10^8*, 2000*
J. Franco, E. Terlevich, O. López-Cruz, and I. Aretxaga, eds.

Dynamical processes, element mixing and chemodynamical cycles in dwarf galaxies

Andreas Rieschick and Gerhard Hensler

Institut für Theoretische Physik und Astrophysik, Universität Kiel, D-24098 Kiel, Germany

Abstract. Since the chemical evolution of galaxies seems to differ between morphological types and deviates in many details from the standard scenario the question has to be addressed when, how and to what amount metal-enriched ejecta from Supernovae and Planetary Nebulae polute their environment. Since recent observations of dwarf galaxies show no significant metal abundance gradients throughout the galaxies while enhancement of metals happens in isolated HII regions, an effective mixing process has to be assumed. Chemodynamical evolution models can provide a possible explanation by demonstrating that strong evaporation of gas clouds by hot gas and following condensation leads to an almost perfect mixing of the gas. We focus on the different phases of chemodynamical evolution that are experienced by a representative dwarf irregular galaxy model and present a quantitative analysis of the chemodynamical gas flow cycles.

1. Introduction

Observations of dwarf galaxies show no significant metal abundance gradients throughout the galaxies (Kobulnicky, Kennicutt, & Pizagno 1999; van Zee et al. 1998). A possible mechanism suggested by Tenorio-Tagle (1996) is the mixing of metal-enriched blow-out gas with fresh matter from the environment of the galaxy. After Supernovae (SNe) have caused an outflow of matter (depending on the mass of the galaxy; see Mac Low & Ferrara, 1998), the hot gas cools, condenses and falls back into the galactic body.

The moderate-to-low stellar metallicities in dwarf elliptical galaxies (dEs) and the related dwarf spheroidals (dSphs) suggest that extensive gas loss has occured during their evolution by means of SNe-driven galactic winds (Larson 1974; Dekel & Silk 1986). Current starburst dwarf galaxies (SBDGs) are characterized by superwinds (Marlowe et al. 1995) or by large expanding X-ray plumes which are often confined by swept-up Hα shells. Yet many dSph galaxies show not only a significant intermediate-age stellar population (Hodge 1989; Grebel 1997), but also more recent star formation (SF) events (Smecker at al. 1994; Han et al. 1997) indicating that gas was partly kept in the systems. On the other hand, gas infall might also cause a new SF episode as in NGC 205 (Welch, Sage, & Mitchell 1998). In several SBDGs large HI reservoirs envelope the luminous galactic body (e.g. NGC 4449: Hunter et al. 1998; I Zw 18: van Zee et al. 1998; NGC 1705: Meurer, Staveley-Smith, & Killeen 1998) and obtrude that the starburst is fueled by enhanced infall. Since the infall rate cannot yet be

evaluated observationally the task for evolutionary models is to investigate the efficiency of SF and its according gas consumption.

2. The Model

2.1. The chemodynamical description

Because of their low gravitational energy dwarf galaxies are strongly exposed to the energetic impact from processes like stellar winds, supernovae or even stellar radiation. When investigating gas mixing by large-scale dynamics and by small-scale exchanges it is necessary to distinguish between the dynamically separated gas components: the dense cloudy medium (CM) and the hot dilute intercloud medium (ICM). To account for differences in energy and timescale of the stellar yield an evolutionary code also has to divide stars into different stellar mass components: high-mass stars (HMS), intermediate-mass stars (IMS) and the not yet evolved low-mass stars (LMS).

The evolution calculation presented here was performed using our chemodynamical evolution code CoDEx, a two dimensional grid-based axisymmetrical evolution code including matter, momentum and energy equations of all relevant processes in a self-consistant way. A detailed description can by found in Samland, Hensler & Theis (1997). Differing from the specifications given there recent HMS yields by Woosley & Weaver (1995) are used which provide secondary nitrogen production (and a small amount of primary nitrogen production). Also, for consistency, the most recent IMS models by van der Hoek & Groenewegen (1997) have been applied.

Contrary to simple chemical evolutionary models that do not distinguish between CM and ICM and therefore have to parameterize separation and mixing of elements and possible selective outflow from the galaxy, the chemodynamical description allows to trace the flow and mixing of metal enriched matter in a self-consistent way.

2.2. Initial conditions

We assume that the protogalactic gas cloud given by a Plummer-Kuzmin model (Satoh 1980) has been formed in a cosmological CDM scenario but was prevented from cooling by the metagalactic UV radiation field (Kepner, Babul, & Spergel, 1997). Not before this background radiation drops, the protogalactic gas cloud can cool due to recombination and subsequently collapes.

The total numerical grid size is 20 *kpc* x 20 *kpc*, the spatial resolution in the central parts amounts to almost 100 *pc*. The evolved numerical model starts with a baryonic mass of about 10^9 $M_\odot$. A static dark matter halo according to Burkert (1995) with a mass of $10^{10} M_\odot$ is added. This model is aimed to represent a dwarf irregular galaxy (dIrr).

3. Results

3.1. Dynamical phases of the evolution

For analytical purposes we devide the model galaxy into four equidistant zones of radial extent of 0.5 *kpc* along the galactic plane up to 2.0 *kpc* and with a z-height of 1.0 *kpc*. The four zones represent tori due to the axisymmetrical grid.

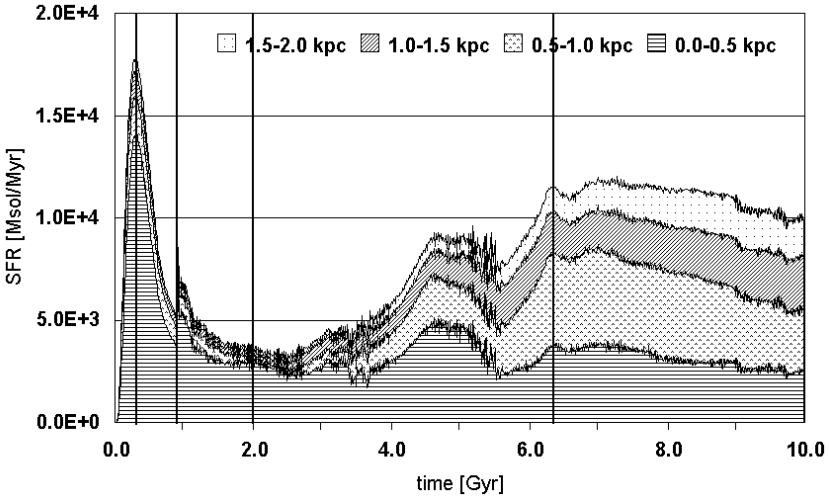

Figure 1. Star formation history of the $10^9 M_\odot$ chemodynamical dIrr model in units of $M_\odot/Myr$ for different radial zones in the equatorial plane. The absolute values correspond to the differences between two curves. The vertical lines devide the different evolutionary phases described in the text.

For consistency we use this scheme throughout the whole evolution, even when the model galaxy changes its shape (e.g. by the settling of a disk-like structure in the galactic plane).

In Figure 1 the SF history for these four zones is plotted. The four curves are stacked, i.e. the uppermost curve is the sum of all four zones. An analysis of the model's kinematics (Rieschick & Hensler, in prep.) implies five distinct dynamical phases of evolution that are indicated in Fig. 1 by vertical lines.

*Collapse phase (*0 - 0.3 *Gyr):* The protogalactic gas distribution is dynamically stable but cools and collapses. The net gas infall rate amounts to $3.2 \cdot 10^{-1} M_\odot/yr$ leading to a central density increase by a factor of 100. Thus the SF rate rises steeply according to its quadratic dependence on the CM-density. The succeeding supernova type II (SNII) explosions starting with a time delay of about one Myr smooth the further collapse of the CM. The peak in CM density is reached after about 300 Myr with a total SF rate of $1.8 \cdot 10^{-2} M_\odot/yr$.

*Post-collapse phase (*0.3 - 0.8 *Gyr):* Evaporation and gas outflow triggered by SNeII lead to further reduction of CM density down to 1/4 of the maximum value. The net gas loss rate averaged over this phase amounts to $6.6 \cdot 10^{-2} M_\odot/yr$. A second much smaller bounce occurs until an equilibrium between gravitation and gas pressure is reached.

*Transitional phase (*0.8 - 2.0 *Gyr):* In this phase the dynamical structure of the model galaxy changes completely. While during the collapse and the post-collapse phase the inward or outward motions, respectively, show almost coherence, now they differ locally and the SF splits into several small regions. This process is accompanied by both decreasing total gas density and total SF.

*Turbulent phase (*2.0 - 6.2 *Gyr):* Two different zones have formed: the central part with a radius of about 0.5 *kpc* and a thick disk in the range between 0.5 and 2 *kpc* distance from the galactic center. These two parts follow separate

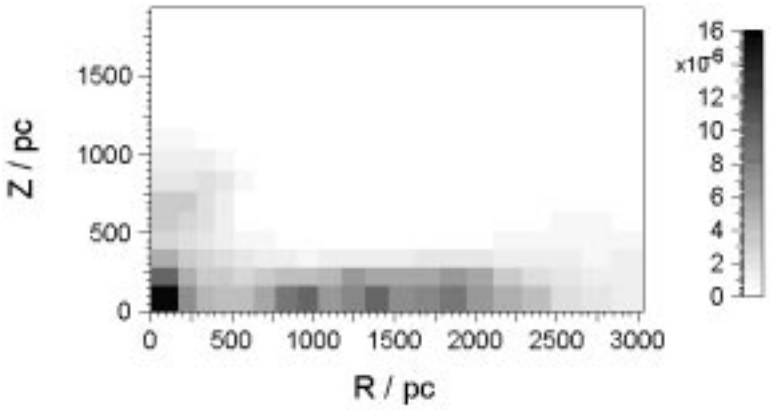

Figure 2. Star formation rate at 8.0 *Gyr* in the single numerical grid cells in units of $M_{\odot}/(Myr \cdot pc^3)$.

paths in SF history. While the central SF rate stays almost constant, the disk SF rate increases nearly by a factor of ten in three steps. Thus the outer zones' SF rate reaches more than $^2/_3$ of the total value while it has been only about 20% before. Regularly this zone splits into a few separate SF regions (Hensler & Rieschick 1999) while SF is wandering outwards in the disk to larger radial distances because a growing number of gas clouds is accreted there due to infall.

Irregular phase (> 6.2 Gyr): A global quasi-stability seems to be reached now, even though the SF in the outer parts of the galaxy happens in shortly living patches. Due to the smaller gas density the exchange with the surrounding is larger than in the central part leading to a non-existing abundance gradient. Because of the incoherence and inhomogenities of dynamics and local regions we denote this phase as "irregular". Figure 2 shows the SF rate at 8.0 *Gyr* as an example. While the highest SF rate per volume ($1.6 \cdot 10^{-6} M_{\odot}/[Myr \cdot pc^3]$) exists in the center of the galaxy, three destinct SF regions with SF rates of about $^1/_2$ of the previous value are visible in the disk. The SF decreases slightly due to less infalling CM gas from the depleted HI reservoir.

3.2. The gas flow cycle

Especially when studying the chemical evolution of galaxies the mixing and exchange processes between gas phases become important. Matter is expelled by SNe as hot dilute gas (ICM) and can return as clouds of cold gas (CM) if it is gravitationally bound. The gas changes its state from ICM to CM by condensation on the surface of gas clouds or vice versa by evaporation.

In Figure 3 we have analyzed the mass flow treated in chemodynamics between the different components averaged between $6.2 - 10.0$ *Gyr* over a cylinder with $r = 2$ *kpc* and $z = 1$ *kpc*. From the mass flow rates one can distinguish between an outer and an inner cycle. The outer one is produced by infall of CM. From this about 24 % is consumed by means of SF where 10 % is almost instantaneously rejected by HMS. The inner cycle represents SF and stellar evolution and, therefore, contains different timescales.

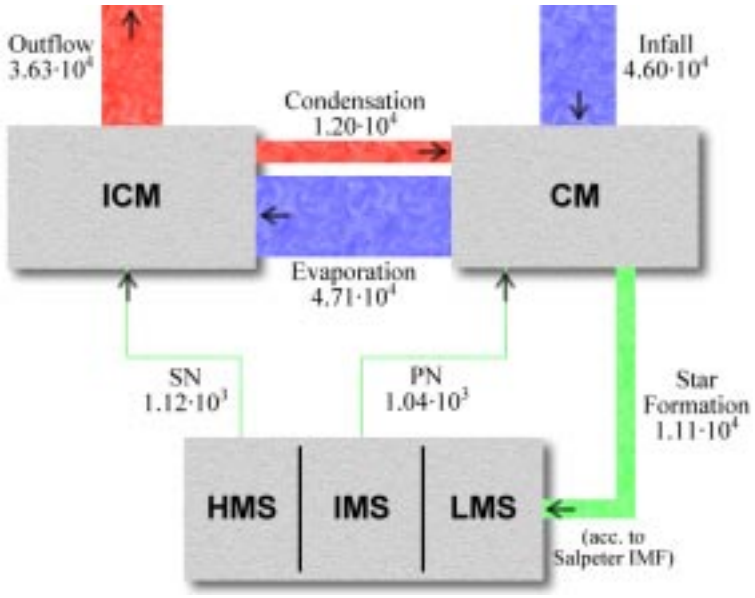

Figure 3. Flow of matter between the components in the chemodynamical dIrr model. The diagram shows the temporal average over the interval 6.2 to 10.0 Gyr (the irregular phase, see text) for a radius of 2.0 kpc and a z-height of 1.0 kpc, i.e. the whole visible galaxy). All numbers are in units of $M_{\odot}/Myr$.

The production of a minor fraction of hot ICM by SNe II leads to evaporation of remaining CM and escapes from the galactic body as outflow as a consequence of its high energy content. Significantly, almost 80 % of the infall is immediately converted into outflow by only 3.0 % of gas that has gone through the stellar cycle and is puffed up by stellar energy release. The full evaporation rate can exceed the infall rate because shell sweep-up leads to fragmentation and cloud formation in addition to a small amount of condensation.

We emphasize that even though a large amount of the outflowing gas is gravitationally unbound and leaves the galactic body, the metals produced in HMS are for the most part kept in the outer gas flow cycle by mixing ICM with continuously infalling clouds. As a result of this mechanism only a few percent of the metals leave the gravitational field of the galaxy with the outflowing ICM. While this mixing itself happens on a timescale of about 20 Myr, the complete cycle of metal enrichment takes almost 1 Gyr because of the low infall velocity at later evolutionary stages. In contrary, the inner cycle leads to an efficient self-enrichment of SF regions within 10 Myr (see also Skillman, Dohm-Palmer, & Kobulnicky, 1998). The outer enrichment timescale would be reduced significantly, however, in a scenario of a rapidly infalling intergalactic gas cloud.

This interaction scheme is running through all dynamical phases with different amounts but nearly the same mass flux ratios. During the collapse phase the infall rate is larger leading to intensive accumulation of matter in the CM and stellar components. In the post-collapse phase the CM density is even decreasing.

4. Conclusions

In the previous section we have shown that a constant infall of metal-poor matter from the enveloping "HI reservoir" drives a permanent gas mixing cycle keeping SNe-produced metals effectively in the gravitational field of the galaxy. Since recent deep HI observations of dIrrs and SBDGs have discovered an increasing number of large gas envelopes, i.e., of enormous gas reservoirs circling or accumulating around the visible body of the BCDGs, the relevance of infall episodes for the DG evolution is obvious and serves as the most promissing explanation for their observed abundances (see Hensler, Rieschick, & Köppen, 1999).

Additionally we demonstrate by chemodynamical models that the SF cycle (Fig. 3) is triggered by only a small fraction of infalling matter, but produces sufficient energy to cause major evaporation and to drive more than 3/4 of the infalling gas, incorporated into the ICM, as a galactic outflow back into an outer long-term cycle. Chemodynamical models can provide a fundamental insight into strong interactions between dynamical and energetical processes that happen in these sensitively balanced systems of low gravitational energy.

Acknowledgments. We gratefully acknowledge cooperation and discussions with J. Köppen and Ch. Theis. A.R. is supported by the *Deutsche Forschungsgemeinschaft* under grant no. He 1487/23-1. The numerical calculations have been performed at the computer center of the University of Kiel and the NIC in Jülich.

References

Burkert, A. 1995, ApJ, 447, L25
Dekel, A., & Silk, J. 1986, ApJ, 303, 39
Grebel, E. 1997, Rev. Mod. Astron., 10, 29
Han, M., et al. 1997, AJ, 113, 1001
Hensler, & G., Rieschick, A. 1999, in Proc. XVIII Rencontre de Moriond, *Dwarf Galaxies and Cosmology*, eds. T. X. Thuan et al. (Gif-sur-Yvettes: Frontiéres), 461
Hensler, G., Rieschick, A., & Köppen, J. 1999, in *The Evolution of Galaxies on Cosmological Timescales*, eds. J. E. Beckman & T. J. Mahoney, ASP Conference Series, Vol. 187, 214
Hodge, P. W. 1989, ARA&A, 27, 139
Hunter, D., et al. 1998, ApJ, 495, L47
Kepner, J. V., Babul, A., & Spergel, D. N. 1997, ApJ, 487, 61
Kobulnicky, H. A., Kennicutt, R. C., & Pizagno, J. L. 1999, ApJ, 514, 544
Köppen, & J., Edmunds, M. G. 1999, MNRAS, 306, 317
Larson, R. B. 1974, MNRAS, 169, 229
Mac Low, M. M., & Ferrara, A. 1999, ApJ, 513, 142
Marlowe, A. T., Heckman, T. M., Wyse, R. F. G., & Schomer, R. 1995, ApJ, 438, 563
Meurer, G. R., Staveley-Smith, L., & Killeen, N. E. B. 1998, MNRAS, 300, 705
Satoh, C. 1980, PASJ, 32, 41
Samland, M., Hensler, G., & Theis. Ch. 1997, ApJ, 476, 544
Skillman, E. D., Dohm-Palmer, R. C., & Kobulnicky, H. A. 1998, in *The Magellanic Clouds and Other Dwarf Galaxies*, proc. of the Bonn/Bochum-Graduiertenkolleg Workshop, eds. T. Richler & J. M. Braun, Shaker Verlag, Aachen, p. 77
Smecker-Hane, T. A., et al. 1994, AJ, 108, 507
Tenorio-Tagle, G. 1996, AJ, 111, 1641
van den Hoek, L. B., & Groenewegen, M. A. T. 1997, A&AS, 123, 305
van Zee, L., Westphal, D., Haynes, M. P., & Salzer, J. J. 1998, AJ, 115, 1000
Welch, G. A., Sage, L. J., & Mitchell, G. F. 1998, ApJ, 499, 209
Woosley, S. E., & Weaver,T. A. 1995, ApJS, 101, 181